J. Phys. IV France **11** (2001)
© EDP Sciences, Les Ulis

Effect of double-layers formation on the deposition of microcrystalline silicon films in hydrogen diluted silane discharges

A. Hammad, E. Amanatides, D.E. Rapakoulias and D. Mataras

Plasma Technology Laboratory, Department of Chemical Engineering, University of Patras, P.O. Box 1407, 26500 Patras, Greece

Abstract: The effect of the double layers formation on the gas-phase composition of SiH_4/H_2 discharges and the deposition rate of microcrystalline silicon thin films has been investigated by applying mass spectrometric and film growth measurements. Spatially Resolved Optical Emission Spectroscopy has been used for the detection of the appearance of this additional electron heating mechanism that in the present conditions results from the variation of either the discharge power or the total gas pressure. The experimental results have been in all cases combined to a gas phase and surface simulator of SiH_4/H_2 discharges allowing thus the discussion for the rather limited effect of this mechanism on the deposition process of μc-Si:H thin films.

1. INTRODUCTION

Hydrogenated microcrystalline silicon (μc-Si:H) prepared by plasma-enhanced chemical vapor deposition (PECVD) has attracted special attention for its application in stable thin-film solar cells [1] due to the fact that it has unique electronic properties compared to crystalline or amorphous silicon [2]. The most common technique used for depositing μc-Si:H thin films is from highly diluted SiH_4 in H_2 discharges [3]. An optimization of this process is only possible by fully understanding the production mechanism of charged particles and radicals, which are closely related to the primary plasma electron heating mechanisms.

Double layers formation can occur in hydrogen or hydrogen rich discharges as a result of another electron heating mechanism besides the well known wave riding heating which usually prevails in plasma deposition conditions. Since the first report by Mutsukura et al. [4] who observed the presence of two distinct emission peaks in front of both electrodes in H_2 glow discharges, a number of studies have been carried out in order to investigate the origin of these double layers in electropositive gases [5-9]. The most probable cause of this phenomenon is the occurrence of a field reversal in the sheath region in a part of the RF period [9]. However, although these studies have helped a great deal in understanding the mechanism that leads to the double layer formation, they were mainly focused on the physical processes that are responsible for the appearance of the additional heating mechanism. This is also the case for the two existing studies [5,6], where discharges of gas mixtures commonly used for the deposition of thin films (highly diluted SiH_4/CH_4 in H_2) have been investigated. No attempt has been made to associate the double layer mechanism to the main processes leading to the film growth.

This is the basic purpose of this work, where the effect of the double layer formation on the deposition of microcrystalline silicon thin films, is reported. The investigation has been performed, in highly diluted SiH_4 in H_2 13.56 MHz discharges, by varying the applied peak-to-peak voltage (150Volt – 400 Volt), at two total gas pressures of 0.5 Torr and 1 Torr. The appearance of double layers in front of the RF electrode has been recorded, using Spatially Resolved Optical Emission Spectroscopy (SROES). The variation of the effective power consumed in the discharge resulting from the change of both the applied voltage and the total pressure, was measured using an accurate method based on the Fourier transform of voltage and current waveforms, as described in detail in Ref. [10].

Furthermore, the impact of the additional electron heating mechanism on the total SiH_4 consumption has been investigated by mass spectrometry, while at the same time the film growth rate has been recorded in situ using Laser Reflectance Interferometry.

Finally, the experimental results concerning the total SiH_4 consumption were used as input in a simulator of the gas-phase and surface chemistry of SiH_4/H_2 discharges [11] and the effect of the

additional electron heating mechanism on the μc-Si:H deposition rate in the present experimental conditions, was thoroughly examined.

2.EXPERIMENTAL

The experiments were performed in a 160 mm in diameter cylindrical parallel plate reactor equipped with four quartz windows suitable for spectroscopic observations. Details concerning the design of the cell can be found elsewhere [12]. In these series of experiments, the electrodes are cylindrical 55mm in diameter and the interelectrode distance is fixed at 25mm. The pressure is adjusted by a downstream throttling valve, while upstream mass-flow controllers are used to set the flow rate.

A schematic diagram of the experimental setup used for the spatially resolved optical emission measurements can be found in Ref. [12]. Briefly, two 0.5mm slits with a 10 cm distance between them and a lens with a 5.5 cm focal length are used to collect a 0.5 mm wide slice of the discharge light onto the entrance slit of a 1m JY-THR1000 monochromator. The chamber is based on a carriage slider permitting the recording of axial spatial emission profiles by moving the cell perpendicularly to the static slit-lens arrangement.

A schematic diagram and details of the electrical connections used for power and impedance measurements, based on a method that has been developed by this group, can be found elsewhere [10]. Briefly, the rf electrode surrounded by a ground shield is powered by an ENI ACG-3 13.56 MHz generator through an *L*-type matching network. A FCC model F-35-1 current probe and a Hameg HZ53 100:1 attenuating voltage probe are used to transfer the current and voltage waveforms measured outside the chamber to a LeCroy 9400 digital oscilloscope. The equivalent current and voltage waveforms on the powered electrode are then calculated using an equivalent circuit with experimentally determined physical components. The most important characteristic of this equivalent circuit is that includes resistive losses in the actual circuit, which has proven to improve drastically the accuracy of the method.

In addition, Silane consumption was determined using a Hidden Analytical (type HAL 301) mass spectrometer connected at the reactor pumping outlet[13]. Finally, the deposition rate was monitored in-situ at a substrate temperature of 250 C, using in-situ Laser Reflectance Interferometry.

Special care was taken in all experiments to monitor particle formation in the gas phase by using a laser light scattering technique as described in Ref. [14]. Through this method it was observed that in highly diluted silane discharges particles are trapped in downstream afterglow regions and do not appear in the plasma sheath boundary, as is also found in other recent studies [15]. These observations suggest that particle monitoring should always be applied in silane containing discharges to insure particle free conditions.

3.RESULTS AND DISCUSSION

The effect of the double layer formation on the radical production, total SiH_4 consumption and μc-Si:H growth rate has been studied at two total gas pressures (0.5 Torr and 1 Torr), in 13.56 MHz highly diluted SiH_4 in H_2 discharges. Two different SiH_4 in H_2 gas mixtures were used (2/150 and 1/150 respectively) in order to maintain a constant silane concentration as pressure increases from 0.5 to 1 Torr. At each pressure, the applied peak-to-peak voltage was varied from 150 V to 400 V. At the same time the variation of the power dissipated in the discharge due to the change of the applied peak-to-peak voltage was monitored using the method described in the experimental section.

In fig. 1(a) and 1(b) are presented the time-averaged emission profiles resulting from one-electron impact dissociative excitation of silane towards SiH ($A^2\Delta$) for the pressures of 0.5 Torr (fig. 1(A)) and 1 Torr (fig.1(b)) under the experimental conditions mentioned above. The most striking feature of the spatial emission profiles is that by increasing the voltage above 250 V in the 0.5 Torr case and above 200

V in the 1 Torr case, a new emission peak appears near the powered electrode. This observation is consistent with the double layer formation, which occurs in hydrogen or hydrogen rich discharges as a result of an additional electron heating mechanism.

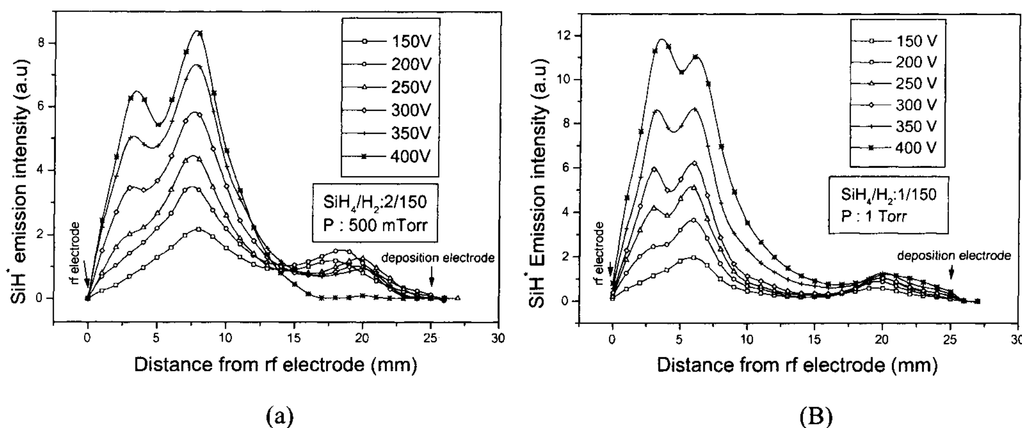

Figure 1. Spatial emission profiles of SiH^*($A^2\Delta \rightarrow X^2\Pi$) intensity (a) for SiH_4/H_2 ratios 2/150 and for a total pressure of 0.5 Torr and (b) for SiH_4/H_2 ratios 1/150 for a total pressure of 1 Torr. The peak-to-peak voltage is varied from 150 V to 400 V.

The existence of the first (leftmost) peak is representative of the establishment of an electric field in the powered sheath, responsible for the electron acceleration in this region. On the other hand, the second emission peak corresponds to the outcome of the effective collisions of electrons that have gained energy by interacting with the oscillating powered electrode sheath of the. The maximum intensity position of the first peak is located 4 mm away from the powered electrode for the two cases and is independent of the excitation voltage, while the second peak presents a maximum at 8 mm and 7 mm for fig.1 (a) and fig.1 (b) respectively. In both figures is also observable the less pronounced grounded sheath electron heating mechanism, the relative importance of which drops with increasing of pressure.

In addition, the increase of the rf voltage markedly enhances the double layer effect. In the high pressure case (fig 1(b)) the intensity of the first peak first reaches the second peak and then it becomes larger than the second peak for 350 V and 400 V respectively.

The changes on the electron heating mechanisms are normally expected to affect the total silane consumption, as electron impact is a very important dissociation path. Thus, in fig. 2(a) is plotted the variation of silane consumption as a function of the discharge power for the two cases of high and low pressure, to demonstrate this effect. The increase of the power density up to 75 mW/cm^2 leads to an enhancement of the measured SiH_4 consumption in both cases, while further increase of the power for the 1 Torr case has almost neglible effect on SiH_4 dissociation. In addition, the increase of pressure increases SiH_4 consumption for the entire range of power densities used. The present data can be interpreted by taking into account the changes in the mass transport mechanisms of the gas in the plasma reactor that depend on the increase of pressure.

Under the present experimental conditions, the plasma reactor behaves as an almost perfectly stirred tank reactor where the SiH_4 residence time τ_r in the interelectrode space can be calculated using the expression:

$$\tau_r = \frac{PA_f d}{Q}, \tag{1}$$

where P is the total discharge pressure, A_f is the reactor cross-section, d is the interelectrode distance and Q is the flow rate. Since in the present experimental set the terms A_f, d, and Q were maintained constant the residence time in the reactor increases directly with pressure thus enhancing the probability of SiH_4 dissociation.

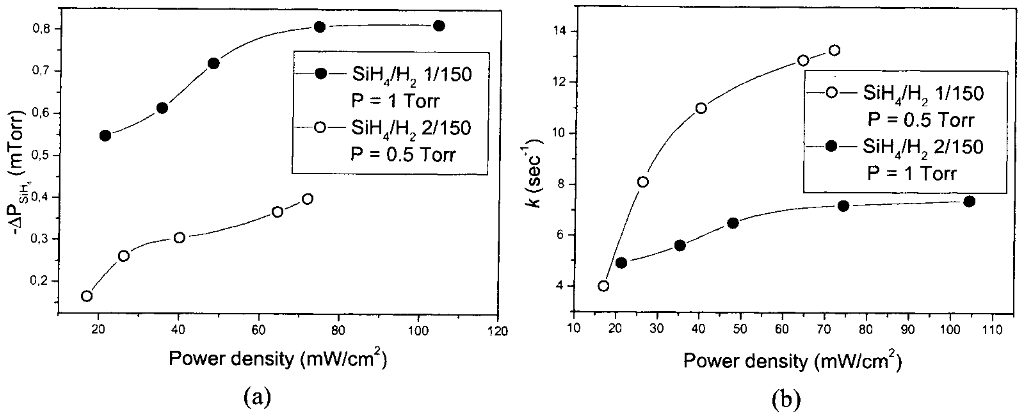

Figure 2. (a) Silane consumption as a function of the power density and (b) SiH_4 dissociation rate as a function of the power density at the two pressures of 0.5 Torr and 1 Torr.

On the other hand, the increase of pressure also enhances the participation probability of radicals in secondary gas-phase reactions relative to their diffusion towards the reactor surfaces. The consumption of the various species by secondary reactions relative to their diffusive transport, can be tested by using the simple term:

$$\frac{k_{\sec}[SiH_4]d^2}{D_n}, \quad (2)$$

where D_n is the diffusion coefficient of the specie n, k_{sec} is the dissociation rate constant of the secondary reactions and $[SiH_4]$ is the silane density in the gas mixture. The increase of pressure will reduce the diffusion coefficient and enhance the rate of most of the radical insertion reactions into silane [16], thus favoring SiH_4 consumption through secondary reactions.

Although the qualitative discussion presented above can explain rather well the effect of pressure on silane consumption the gas phase chemistry of SiH_4/H_2 discharges is much more complicated. Therefore, in order to have a better estimation of the different silane dissociation paths a gas phase simulator has been used. The model simulates highly diluted SiH_4 in H_2 discharges in a parallel plate reactor, involving gas-phase chemistry, mass-transfer and substrate-plasma interaction [11]. The model uses as input the total silane consumption and the spatial distribution of the SiH_4 electron impact dissociation rate, ensuring thus the correct prediction of silane electron induced dissociation in space and as a total. With these inputs, the model predicts the deposition rate, the radical fluxes towards surfaces and the dissociation rate of SiH_4.

The application of the model in the present experimental conditions for the calculation of the dissociation rate k of SiH_4 towards neutral radicals is shown in fig. 2(b). A no simple relation between dissociation rate and power density is obtained while in contrast to the previous observation concerning SiH_4 consumption, k is smaller in the case of high pressure than in the low pressure case except for power densities less than 20 mW/cm^2. In 1 Torr, the drastic increase of power from 47.9 to 104.3 mW/cm^2 is not followed by an analogous increase of k, which is almost constant over this range. It is worth noting that for the same increase of power, silane dissociative excitation, which is a process with much higher electron energy requirements compared to silane dissociation towards radicals, has been enhanced through the formation of double layers (fig. 1(b)). This dissimilar behavior between silane dissociation and excitation can be attributed to the changes on the distribution of the power consumed in electron-molecule collisions and in ion acceleration. Processes with higher energy threshold seem to be favored

under these conditions while the fraction of power dissipated in ion acceleration is expected to increase with power [17].

Since the production of radicals is closely related to the formation of the film precursors, the reduction of silane dissociation rate with pressure is also expected to affect the film growth rate. To verify this, the variation of the experimentally measured deposition rate as function of the power density is shown in the fig. 3(a) and 3(b), for 0.5 Torr and 1 Torr, respectively. The deposition rate varies from 0.03 Å/sec to 0.12 Å/sec for the high-pressure case while lower pressure presents always-higher deposition rate varying from 0.08 Å/sec to 0.2 Å/sec. Thus, despite the existence of double layers (as an additional electron heating mechanism) the observed deposition rates are generally very low, due to the large interelectrode gap and the low fraction of SiH_4 in the gas mixture. Previous work of this group has revealed the importance of both the interelectrode gap [18] and the silane partial pressure [19] on the deposition rate and this seems also to be the case under the conditions of double layer formation.

The fact that the deposition rate is always lower for 1 Torr than for 0.5 Torr is the result of at least three reasons. First, as shown in figure 2(b) the rate of silane dissociation k is lower for the high-pressure case inducing a decrease of the rate of radical's production. Second, the maximum rate of the production of film precursors is displaced towards the powered electrode due to the decrease of the sheath width at the higher pressure. Thus, the contribution of radicals that have quite small diffusion length, to the total film growth will decrease in the 1 Torr case. Finally the diffusion of all radicals towards surfaces, which is the main mechanism of radicals transport, will be hindered at the high pressure.

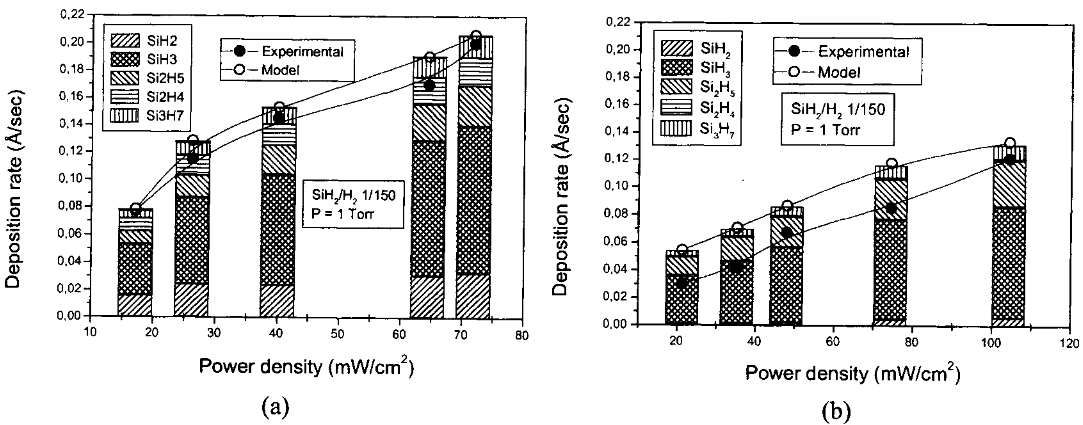

Figure 3. (a) Deposition rate as a function of the discharge power for total gas pressure of 0.5 Torr and (b) for total gas pressure of 1 Torr. The deposition rate predicted by the model and the contribution of the main radicals to the film growth are also included.

The validity of the above explanations can be also checked, using the model predictions of the deposition rate. Thus, in fig. 3(a) and 3(b) together with the experimental measurements are also included the model anticipations concerning the deposition rate and the contribution of the main radicals to the film growth. A quite good agreement between model and experimental results can be observed and this allows discussing the contribution of the main radicals to the film growth. More precisely, silyl (SiH_3) radical dominates by far all other species, contributing to almost 50% of the total film growth under the present conditions. A no neglible contribution is also attributed to polysilyl radicals (Si_2H_5, Si_3H_7) while the participation of highly sticking radicals (SiH_2, Si_2H_4) remains in all cases less than 35% and decreases with increasing pressure.

This domination of low sticking radicals against highly sticking ones to the total film growth can be understood by taking into account their different gas phase and surface reactivity. These differences are reflected on the spatial distribution of SiH_2 and SiH_3 radical densities that result from the mass balance of these species in the discharge and is presented in fig. 4 for both pressures of 0.5 Torr and 1 Torr for the same applied voltage (400 V). Comparing the spatial distribution of SiH_2 and SiH_3 for the same pressure,

one can observe that the density of SiH_3 radicals peaks further from the powered electrode than that of SiH_2, while the density of SiH_3 in every point of the interelectrode space is in both pressures much higher than SiH_2. In addition, the profile of SiH_3 radical is determined by the diffusion and the consumption of this radical at the surfaces, while the profile and the density of SiH_2 are determined by its fast consumption in the gas phase.

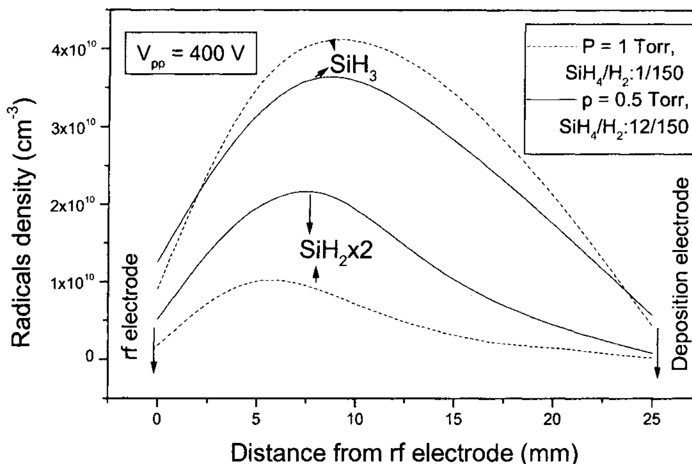

Figure 4. The spatial distribution of SiH_3 and SiH_2 radicals for constant peak-to-peak voltage of 400 V.

On the other hand the increase of pressure affects both the location of radicals maximum densities that are displaced towards the powered electrode and the SiH_2/SiH_3 densities. The displacement of the maximum is strictly related to the decrease of the powered sheath length at 1 Torr, while the effect of pressure on the SiH_2/SiH_3 densities is more complicated. Concerning the SiH_2, the earlier mentioned fast consumption of this radical in the gas phase is enhanced in the high pressure (eq. (2)), resulting to very low densities. As for the SiH_3 radical, which is not very reactive in the gas phase, its density remains rather high in the 1 Torr case as the diffusive losses of this radical are reduced.

Finally, based on the main characteristics of the gas phase chemistry presented above, the effect of the double layers formation on the microcrystalline silicon deposition process can be summarized in two main conclusions. First, it is important to note that the conditions leading to the enhancement of this mechanism were not followed by an analogous increase of the total silane consumption. This observation automatically leads to the conclusion that electron induced silane dissociation towards neutrals is not favored by this mechanism. Second, double layers formation affects the spatial production of these radicals only close to the powered electrode. Thus, the quite large distance between the radical production through this mechanism and the deposition (grounded) electrode limits the effect of the double layers formation on the deposition rate.

Further work is in progress that includes direct monitoring of the production of neutral radicals and deposition rate measurements on the powered electrode, in order to completely clarify the effect of the double layers on microcrystalline silicon deposition process.

4. Conclusions

The existence of double layers in front of the powered electrode has been observed by time-averaged optical emission spectroscopy measurements in highly diluted SiH_4 in H_2 plasmas at two total gas

pressures and various power densities. Mass spectrometric measurements of the total silane consumption have been performed under the same conditions while at the same time the deposition rate has been monitored using Laser Reflectance Interferometry (LRI). The experimental results were in all cases combined to a gas phase/surface simulator, allowing the prediction of SiH_4 dissociation rate and the contribution of each of the radicals to the film growth.

The increase of the power has been found to lead to an enhancement of SiH_4 consumption and of the silane primary dissociation rate for both pressures. Namely, silane consumption increases with pressure, over the entire range of power densities presented here, while at the same time SiH_4 dissociation rate constant decreases. This behavior can be attributed to the higher SiH_4 residence time and to the suppression of the diffusive flux of radicals towards surfaces that enhance SiH_4 consumption through secondary gas phase reactions in the high-pressure case.

The film growth rate has been found to follow silane dissociation rate i.e increases with power and drops with pressure. SiH_3 radical has been found to dominate the film growth, by contributing by more than 50% in both pressures. This has been attributed to the quite large electrode gaps and the low silane contents used in this study that are also responsible for the rather low deposition rates. Indeed, the situation concerning the main film precursor will be drastically changed when decreasing the interelectrode distance [18], where also the effect of the additional electron heating mechanism is expected to be somewhat increased.

References

[1] Wyrch N., Torres P., Goetz M., Dubail S., Feitknecht L., Cuperus J., Shah A., Rech B., Kluth O., Wieder S., Vetterl O., Stiedig H., Benking C. and Wagner H. "Development of inverted micromorph solar cells", Proceedings 2nd World Conference on Photovoltaic Energy Conversion, Vienna, Vol. I, (1998) 467-471.
[2] Schroop R. and Zeeman M.., *Amorphous and Microcrystalline Silicon solar cells,* (Kluwer Academic Publisers, (1998) pp. 42-58.
[3] Matsuda A., J. Non-Cryst. Solids 59&60, (1983) 767-775.
[4] Mutsukura N., Kobayashi K. and Machi Y., J. Appl. Phys. 66 (1989) 4688-4695.
[5] Tochikubo F., Makabe T., Kakuta S. and Suzuki A., J. Appl. Phys. 71 (1992) 2143-2150.
[6] Leroy O., Stratil P., Perrin J., Jolly J. and Belenguer Ph., J. Phys. D: Appl. Phys. 28 (1995) 500-507.
[7] Mahony C., Al Wazzan R. and Graham W., Appl. Phys. Lett. 66 (1995) 263-610.
[8] Graham W. and Mahony C., J.Physique Coll., IV 7 (1997) C4-209-214.
[9] Czarnetzki U., Luggenhölscher D. and Döbele H., plasma Sources Sci. Technol. 8 (1998) 230-248.
[10] Spiliopoulos N., Mataras D. and Rapakoulias D., J. Vac. Sci. Technol. A, 14 (1996) 2757-2765.
[11] Amanatides E., Stamou S., Mataras D., and Rapakoulias D. "Simulation of Plasma Enhanced Chemical Vapour Deposition of microcrystalline silicon based on optical diagnostics" Proceedings of 16th European Photovoltaic Solar Energy Conference, Strasburg 1-5, 2000, in press; Amanatides E., Stamou S., and Mataras D.,submitted to J. Appl. Phys.
[12] Mataras D., Cavadias S. and Rapakoulias D., J. Appl. Phys. 66 (1989) 119-124.
[13] Spiliopoulos N., Mataras D. and Rapakoulias D. E., J. Electrochem. Soc. **144** (1997) pp. 634-640.
[14] Stamou S., Mataras D. and Rapakoulias D., Chem. Phys., 218 (1997) 57-65.
[15] Jelenkovic B., and Gallagher A., J. Appl. Phys. 82 (1997) 1546-1553.
[16] Jasinski J. and Chu J., J. Chem. Phys. 88 (1988) 1678-1687.
[17] Godyak V., Piejak R. and Alexandrovich B., J. Appl. Phys 69 (1991) 3455-3460.
[18] Amanatides L., Mataras D. and Rapakoulias D."Influence of the variation of interelectrode space on the deposition of microcrystalline silicon films in an asymmetric cell" 14th International Symposium on Plasma Chemistry, Prague (1999) 1345-1349.
[19] Amanatides E., Mataras D. and Rapakoulias E. D., Thin Solid Films **383** (2001) pp. 15-18.